pISSN 1229-3008 eISSN 2287-6251
Progress in Superconductivity and Cryogenics
Vol.26, No.1, (2024), pp.14~19 https://doi.org/10.9714/psac.2024.26.1.014

Investigation on the phonon behavior of MgB_2 films via polarized Raman spectra

R. P. Putra, J. Y. Oh, G. H. An, H. S. Lee, and B. Kang*

Department of Physics, Chungbuk National University, Cheongju, South Korea

(Received 7 March 2024; revised or reviewed 28 March 2024; accepted 29 March 2024)

Abstract

In this study, we explore the anisotropy of electron-phonon coupling (EPC) constant in epitaxially grown MgB_2 films on c-axis oriented Al_2O_3, examining its correlation with the critical temperature (T_c) and local structural disorder assessed through polarized Raman scattering. Analysis of the polarized Raman spectra reveals angle-dependent variations in the intensity of the phonon spectra. The Raman active mode originating from the boron plane, along with two additional phonon modes from the phonon density of states (PDOS) induced by lattice distortion, was distinctly observed. Persistent impurity scattering, likely attributed to oxygen diffusion, was noted at consistent frequencies across all measurement angles. The EPC values derived from the primary Raman active phonon do not significantly vary with changing observation angles, followed by that the T_c values calculated using the Allen and Dynes formula remain relatively constant across all polarization angles. Although the E_{2g} phonon mode plays a crucial role in the EPC mechanism, the determination of T_c values in MgB_2 involves not only electron-E_{2g} coupling but also contributions from other phonon modes.

Keywords: MgB_2 film, polarized Raman, critical temperature, EPC

1. INTRODUCTION

Magnesium diboride (MgB_2) is a hexagonal metallic material that is composed of two separate layers of magnesium and boron that stack on top of each other [1, 2]. This simple structure of MgB_2 classified as a BCS type phonon-mediated superconductor with unexpectedly higher critical temperature T_c around ~39 K compared to the other metallic superconductors [1]. Due to its high T_c and simple structure, investigation on its superconducting mechanism and searching for several factors affecting its behavior are still hot topics as MgB_2 becomes essential in replacing the archaic superconductor that has been widely used.

Numerous models, theories, and calculations explaining the superconducting mechanism of MgB_2 have been published [2-9]. According to the band structure calculation [3, 4], MgB_2 has two essential electronic bands that are two-dimensional (2D) p_x and p_y (σ) band, and three-dimensional (3D) p_z (π) band, which forms two cylindrical Fermi surfaces and creates two corresponding superconducting gaps [4]. Each band has a different characteristic such as electrons in the σ band strongly coupled with phonon imprisoned within the lattice, while the π band shows a weak coupling. Since MgB_2 is classified to be owning a strong electron-phonon coupling (EPC) for its superconducting properties, research on how phonon contributes to the T_c behavior is an interesting topic to be studied. Owing to the simple hexagonal structure with the *p6/mmm* space group, several optical modes at the Brillouin zone are predicted for MgB_2 depending on the point of observation [10-12]. Group theory has calculated that MgB_2 has five different phonon modes lying in the Brillouin zone, such as E_{2g} and A_{1g} for active Raman modes, silent B_{1g} mode and two infrareds active E_{1u} and A_{2u} modes [10].

Several reports regarding the possibility of a close relation between lattice, local structure, the behavior of Raman scattering and the T_c values of MgB_2 have been reported [11-13]. The T_c behavior of MgB_2 was explained by the competition between the dominating E_{2g} mode and the other modes reflected in the Raman spectra. The Raman frequency of MgB_2 with different types is affected by several factors such as impurity, lattice strain and stress, which asymmetrically deform either the boron or the magnesium plane. Maintaining the MgB_2 crystal condition with a preferred direction is an advantage of a film form on a suitable substrate, where it can increase the current carrying capacity (J_c) and the upper critical field (H_{c2}) without a degradation of T_c [14].

In this paper, to investigate the relation between the EPC strength and the T_c variation, we report the Raman scattering behavior of the *c*-axis oriented MgB_2 film deposited on Al_2O_3 substrate [15] using linearly polarized Raman measurements at different angles.

2. EXPERIMENTAL DETAILS

MgB_2 films were deposited using a hybrid physical-chemical vapor deposition (HPCVD) technique on the top of the *c*-cut oriented Al_2O_3 substrate. The detailed process

* Corresponding author: bwkang@chungbuk.ac.kr

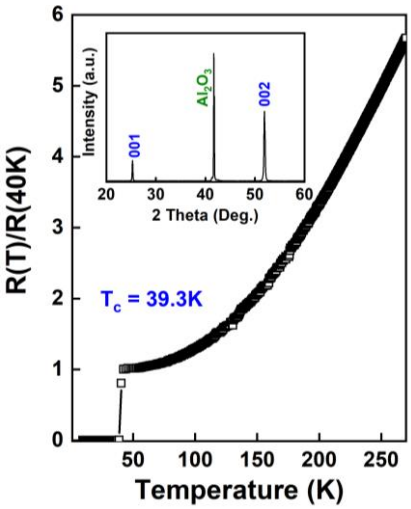

Fig. 1. Normalized resistance curve of MgB_2 film on top of Al_2O_3 substrate. Inset: (Top) XRD data of the deposited sample show highly *c*-axis oriented with only 00*1* and 00*2* peaks are distictly observed .

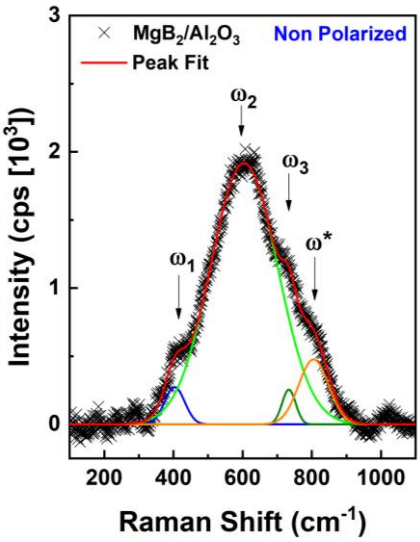

Fig. 2. Background reduced Non-polarized Raman spectra of MgB_2 film on the top of Al_2O_3 substrate at room temperature alongside with gaussian fitting. Additional peak on the high frequency region is detected as impurity peak scattering.

is described elsewhere [13]. To deposit a *c*-axis oriented MgB_2 film on the Al_2O_3 substrate, high deposition temperature around 700ºC was used under 50 torr of H_2 gas at a flow rate of 90 sccm, and then B_2H_6 (10% in H_2) gas at a flow rate of 10 sccm was introduced into the quartz tube chamber for 5 min to start the growth of MgB_2. The deposited MgB_2 film was cooled down to room temperature under a flowing H_2 gas resulting in average thickness around ~800 nm determined from the scanning electron microscope (SEM) cross section image.

Crystal structure of deposited MgB_2 film was examined using X-ray diffraction (XRD) to confirm the epitaxial condition of the sample. The temperature dependence of resistance of the film was measured by standard four-point-probe technique from 297 K down to 10 K. The T_c value was determined from the maximum temperature of dR/dT. Raman scattering measurements were conducted using Raman spectrometer (Nano Photon Raman Touch-model) at room temperature in three different spots with incident laser 532 nm (2.25eV) from range 0 to 1800 cm^{-1}. For polarized Raman scattering measurement, polarized filter in a 15°of interval was used from in-plane 0° to out-of-plane 90°, while the circularly polarized was measured using quarter wave plate (QWP) for two different configurations where the incident, and scattered light measured in a clockwise direction (σ^+ in σ^+ out) or known as Right-Right (RR) and where the incident light measured in a clockwise direction while the scattered light measured in counter clockwise direction (σ^+ in σ^- out) or known as Right-Left (RL).

3. RESULTS AND DISCUSSION

Fig. 1 shows the normalized resistance as a function of temperature measured from 285 K down to 10 K with a RRR to be ~5.8, which is considered to be a clean sample. The T_c value of the sample is determined to be ~39.3 K from the maximum dR/dT. The orientation of the film was confirmed to be highly *c*-axis oriented from the XRD data as in the inset of Fig.1, showing only (001) and (002) peaks indicating that MgB_2 crystal is arranged well on top of Al_2O_3 substrate [15].

Fig. 2 presents the non-polarized Raman spectra measured at room temperature. As generally known, the Raman spectra of MgB_2 consist of three phonon modes, which are the main Raman active phonon spectra located at ~580 cm^{-1}, and two phonon density of states (PDOS) spectra located at ~400 cm^{-1} and ~700 cm^{-1} [11-13]. By employing the convolution Gaussian fitting, the first peak is observed at ~404 cm^{-1}, the second peak probably belonging to the E_{2g} mode is at 604 cm^{-1}, and the third peak at 734 cm^{-1}. Interestingly, an additional peak is observed at 806 cm^{-1} and all the peaks are named as ω_1, ω_2, ω_3 and ω^*, respectively.

The appearance of the additional peak ω^* was reported in the prior reports [13], in which ω^* is considered to belong to impurity scattering due to the oxygen diffusion caused either by ambient condition of the surface or by Al_2O_3 during the deposition of MgB_2 [16-18]. Nevertheless, the appearance of ω^* might not disrupt the phonon behavior of MgB_2.

Angle-resolved polarized Raman spectroscopy (ARPRS) is an important branch of the Raman spectroscopy along with helicity-resolved Raman spectroscopy (HRRS), where we can vary the configuration to alter the incident light of the measurement system, to rotate the polarization light, to rotate the sample in in-plane direction and to apply the quarter wave plate to induce a circularly polarized light [19]. This type of Raman measurement setup has an advantage over the conventional polarized one such that we can use the setup for characterizing the in-plane and out-of-plane phonon modes based on the helicity of Raman scattering. ARPRS can also be used to study the orientation of the Raman tensor by determining the isotropic characteristics of materials [20]. Direct relation between

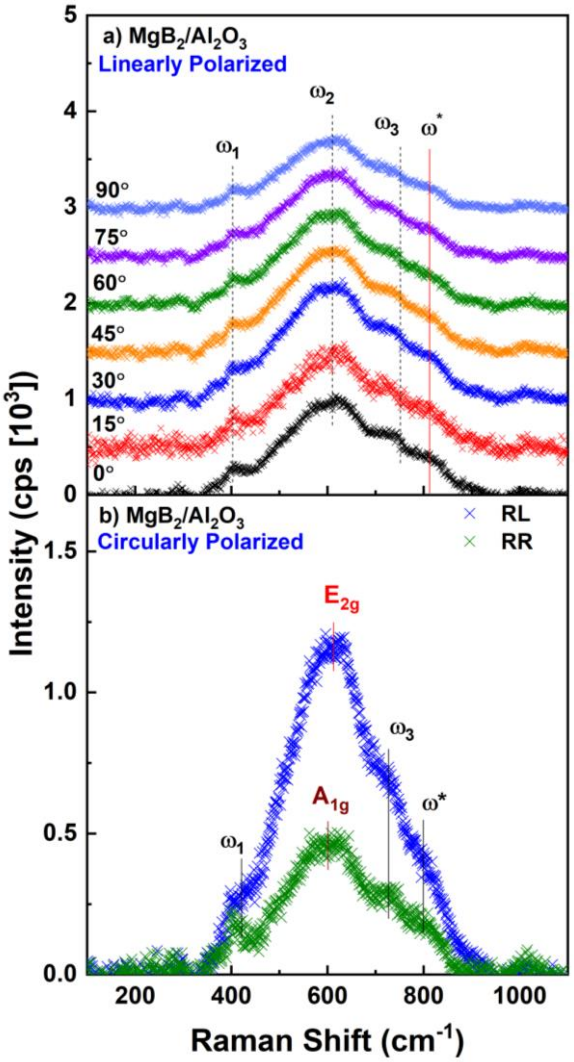

Fig. 3. (a) Linearly polarized Raman spectra of MgB_2 film on the top of Al_2O_3 substrate measured at room temperature from 0° to 90° with a 15° of interval and (b) Circularly polarized Raman spectra with two different configurations of RR (σ^+ in σ^+ out) and RL (σ^+ in σ^- out).

the polarization technique and the superconducting behavior of MgB_2 has not been thoroughly examined yet. Therefore, investigation on the polarization spectra of MgB_2 phonon behavior will bring an insight into how it is related to the strong electron phonon coupling.

The linearly polarized Raman spectra of MgB_2 on top of Al_2O_3 are presented in Fig. 3(a). During the measurement, the angles of incident photon were varied from 0° to 90° with a 15° interval on three different spots and five times measurements were conducted under 10 second of the laser exposure. As can be observed, the behavior of peak positions in the linearly polarized Raman spectra shows a similar pattern to the non-polarized spectra of four peaks detected [10-13, 16-18]. Interestingly, a noticeable difference depending on the measurement angle can be observed in terms of intensity of each main phonon mode ω_1, ω_2, and ω_3. Furthermore, by fixing the frequency value and FWHM of the impurity Raman scattering, we systematically analyze the effects of the main phonon behavior to the strength of electron phonon coupling in MgB_2.

Known to be a hexagonal structure with a stacking 2D layer between magnesium and boron, MgB_2 belongs to the D_{6h} point group in general based on the selection rules [21]. According to the group theory, the symmetries of Raman active modes and the corresponding Raman tensor (R) are described as [22-24]:

$$A_{1g}: \begin{pmatrix} a & 0 & 0 \\ 0 & a & 0 \\ 0 & 0 & b \end{pmatrix}; E_{1g}: \begin{pmatrix} 0 & 0 & 0 \\ 0 & 0 & c \\ 0 & c & 0 \end{pmatrix} \begin{pmatrix} a & 0 & -c \\ 0 & 0 & 0 \\ -c & 0 & 0 \end{pmatrix}$$

$$E_{2g}: \begin{pmatrix} 0 & d & 0 \\ d & 0 & 0 \\ 0 & 0 & b \end{pmatrix} \begin{pmatrix} d & 0 & 0 \\ 0 & -d & 0 \\ 0 & 0 & 0 \end{pmatrix},$$

where the values corresponding to $a - d$ refer to the amplitudes of the Raman tensor element, and both E_{1g} and E_{2g} modes are known to be doubly degenerated. According to the Placzek polarizability approximation, where it can carry out the ratio between the perpendicular component and the parallel components of Raman scattered light, the intensity of Raman scattering (I) can be expressed as the following by using the Raman tensor [23]:

$$I \propto |e_i \cdot R \cdot e_s|^2 , \quad (1)$$

where e_i and e_s are the polarization vectors of incident and scattered light, for linearly parallel polarization configuration where the angle is equal to 0°. The intensities of known Raman active scattering by available matrix are $|a^2|$ for A_{1g}, 0 for E_{1g} and $|d^2|$ for E_{2g} modes. Contrarily, the intensity of Raman active scattering in linearly perpendicular polarization configuration is annihilated except for the E_{2g} mode, which is the value of $|d^2|$ due to its doubly degenerate nature. Otherwise, the value of 0 for E_{1g} indicates that this Raman scattering is unobservable in this experimental setup.

Although, the active Raman mode has been explained and formulated in the group theory, each of observable Raman active mode in our sample hasn't been resolved yet. Following several published reports regarding the Phonon behavior in a conventional polarized angle Raman scattering, A_{1g} phonon mode was observed near the main E_{2g} mode since both phonon modes are coming from the boron plane in- and out-of-plane vibration. In agreement with our linearly polarized Raman measurement, the intensity of ω_2 decreases upon increasing the polarization angle which translates to an elimination of the observable Raman scattering A_{1g} mode close to the E_{2g} mode in perpendicular configuration. To confirm this hypothesis, we performed the HRRS Raman scattering measurement setup was conducted which typically used to assign and resolve the symmetries and chirality of Raman bands.

Fig. 3(b) shows the results of the HRRS Raman spectra measurement with two different configurations, RR (σ^+ in σ^+ out) and RL (σ^+ in σ^- out). As can be seen, the intensity in the RR configuration is lower than that in the RL configuration, which is because that the RR configuration only allows the A_{1g} phonon mode with a value of $|a^2|$ while in the RL configuration, only allowed phonon mode

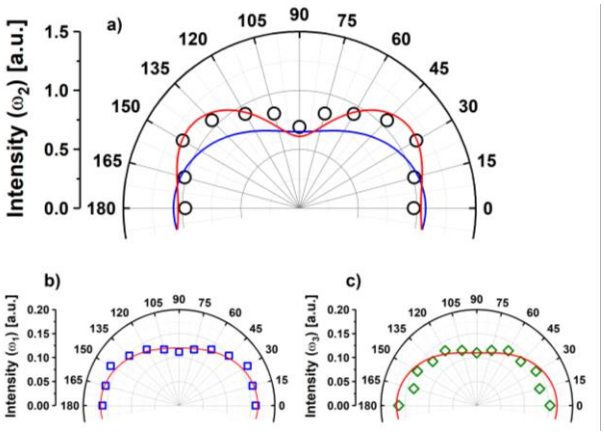

Fig. 4. The polar plot of the integrated intensity of (a) ω_2 followed by theoretical approximation fitting of two phonon-modes combination (blue-line) and three phonon-modes combination (red-line) (b) ω_1 and (c) ω_3 alongside sinusoidal fitting (red-line).

is E_{2g} with the value of $2|d^2|$ according to the group theory and the calculation of the Raman matrix [22, 23]. While we know that the ω_2 phonon mode consists of two Raman active mode A_{1g} and E_{2g} have different behavior of intensity, the other two phonons ω_1 and ω_3 have a quite similar behavior upon those two configurations combined, where a linear and cosine function fits the experimental data. However, due to large linewidth (FWHM) of ω_2, it is difficult to distinguish between A_{1g} and E_{2g} in non-linear and linearly polarized spectra which lead us to treat ω_2 as a phonon combination dominated by E_{2g} mode.

Fig. 4 shows a polar plot of the Raman intensity on three main peaks of ω_1, ω_2, and ω_3. Even though we observe that ω_2 comprises of two different Raman active modes, treating it as one results in a better perspective of how it behaves in respect to the polarization angle. Following the group theory, the behavior of E_{2g} phonon mode appears to be linear such that its intensity maintains the same value across all polarization angles. On the other hand, the A_{1g} phonon mode follows the intensity behavior of $I = A^2 \cos^2\theta$, where A is an amplitude, and θ is representing the linear polarization angle. Thus, the combination of E_{2g} linear equation and A_{1g} cosine equation is presented as the blue line in Fig. 4(a). Unfortunately, our data from the linear polarization Raman scattering do not follow this trend and seem to require an additional sinusoidal fitting function in the Raman tensor [21], which may be originated from the oxygen impurity that affects the condition of boron plane. Otherwise, in order to thoroughly analyze this effect, a detailed measurement using neutron scattering is needed.

Unlike ω_2, the Raman tensors of the other two phonon mode ω_1 and ω_3 in the MgB_2 which is believed to come from the PDOS has not been thoroughly discussed. Furthermore, the intensity of two other main phonon falls in the perpendicular polarization direction which means the PDOS phonon direction follows the behavior of the main phonon ω_2. Since these three phonon modes are closely related to the crystal structure and boron plane condition of the sample, it can clearly be seen that our MgB_2 samples

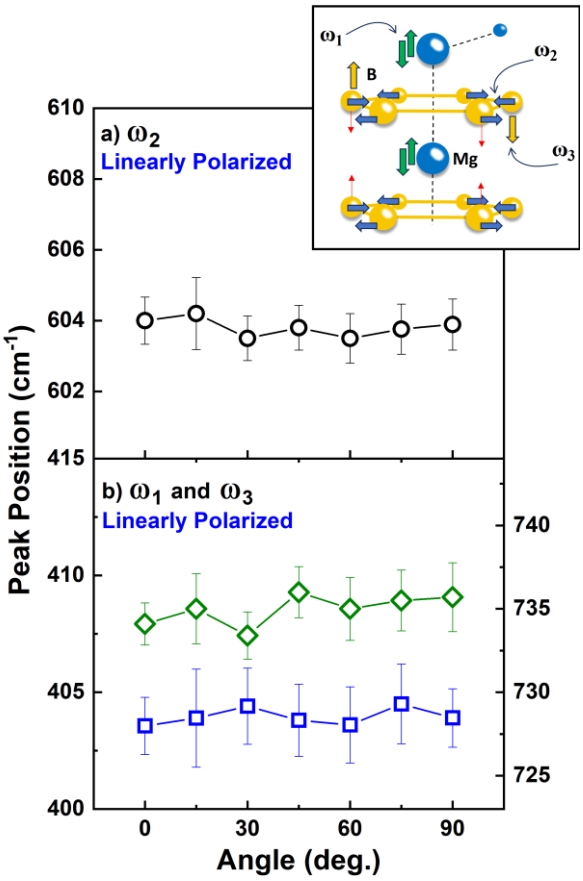

Fig. 5. Raman peak position obtained from the Gaussian fitting of (a) ω_2, (b) ω_1 and ω_3 in respect to the polarization angle. Inset: an illustration of directional phonon modes.

have an anisotropic condition proving several theories that has been published previously [3-7].

The T_c values of phonon mediated superconductor rely on how phonon behaves inside the Brillouin zone of the crystal. The equation of T_c was first published by McMillan and then modified by Allen and Dynes as in the following [25, 26]:

$$T_c = \left\langle \frac{\omega_{log}}{1.2} \right\rangle exp\left(\frac{-1.04(1+\lambda)}{\lambda - \mu^*(1+0.62\lambda)} \right), \quad (2)$$

where $\langle \omega_{log} \rangle = (\omega_1 \times \omega_2^2 \times \omega_3)^{0.25}$ is the averaged phonon frequency [3], μ^* is the Coulomb pseudopotential ranging between 0.1–0.2 in theory [4, 25] and λ represents the EPC constant and λ = 1.29 is used for a single crystal [27].

As stated previously, the T_c variation of MgB_2 was explained by the competition between the main E_{2g} mode and the other modes. As can be seen in Fig. 5, the phonon frequency of ω_2 behaves rather regardless of the polarization angles, followed by ω_1 and ω_3. Thus, employing the polarization method on Raman measurement does not change any observed phonon energy of the phonon modes within the range of error bar. Thus, by employing eq. (2), we calculated T_c's of our sample in respect to the polarization angles and are shown in Fig. 6(a).

Utilizing all phonon frequency ω_1, ω_2, and ω_3 from the

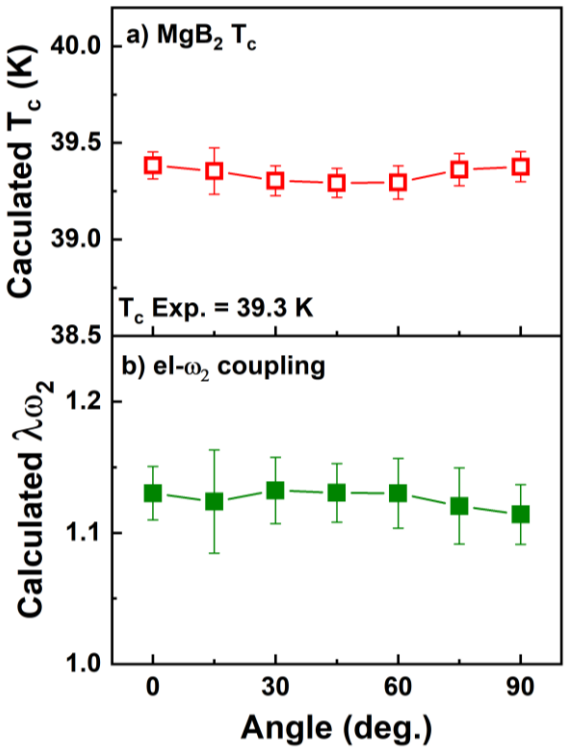

Fig. 6. Calculated T_c and the electron-ω_2 phonon coupling constant taken from the experimental data in respect to the polarization angle.

experiment, we found that the T_c values of our sample do not have any significant change over the polarization angle from the in-plane (0°) to the out-of-plane (90°). Especially, to match with T_c of our sample, a larger value of 0.19 is used for μ^*, which is beyond the reported range of 0.13~0.17 in previous experiments [26], but within the range of the theoretical value [4, 25]. Higher value of μ^* of our sample compared to the other experimental results was assumed to be higher coulomb interaction due to the thickness of our sample being ~800 nm, which can be considered as a bulk sample.

Following several reports published previously, the contribution to the electron phonon coupling in MgB_2 strongly relies on the E_{2g} mode in the ω_2 region along with the A_{1g} mode [22]. While it is difficult to distinguish between E_{2g} and A_{1g}, the coupling of A_{1g} with electron is reported to be far less than that of E_{2g} with electron [28-30]. Thus, we treat ω_2 as the frequency of E_{2g} to calculate the electron- ω_2 coupling constant as following:

$$\lambda_{\omega_{ph}} = \frac{\Gamma}{2\pi N(0)\omega_{ph}^2}, \qquad (3)$$

where $\lambda_{\omega_{ph}}$ is the strength of EPC, Γ is the phonon linewidth obtained from the Gaussian fitting, and N (0) is DOS of the Fermi surface and is an only electronic property explicitly occurring in this equation [31]. In a single crystal MgB_2, N (0) = 0.71 states/eV/cell was used for calculation and considered to be constant [4]. Fig. 6(b) shows the calculated electron-ω_2 coupling constant on each polarization angle. Following the stable behavior of the T_c calculated from the McMillan equation, insignificant change of EPC was also observed, while the value of the EPC from the E_{2g} mode alone is lower than the reported value. This analysis implies that the T_c behavior of MgB_2 relies not only on its Raman active E_{2g} phonon alone, but also on the other two phonon modes. Moreover, it has been demonstrated that T_c of our sample remains unaffected by variations in the measurement angle.

4. SUMMARY

This investigation aimed to observe the phonon behavior within a *c*-axis oriented MgB_2 film deposited on top of an Al_2O_3 substrate, varying the polarization angle. Linearly polarized (ARPRS) and circularly polarized (HRRS) techniques were employed to scrutinize in-plane and out-of-plane phonon behavior, including helicity in Raman scattering and EPC. Non-polarization measurement of the Raman spectra shows that there are three main phonon peaks that can be observed with an additional impurity peak from the oxygen contamination. In addition, the HRRS measurement shows that an additional phonon mode was observed in the ω_2 region. According to group theory, phonon mode ω_2 is a result from a combination of A_{1g} and E_{2g} modes, with E_{2g} believed to have more significant coupling to electrons. Furthermore, the superconducting transition properties of MgB_2 are partly attributed to phonon frequencies and linewidths, particularly the dominant E_{2g} mode. The application of the McMillan equation modified by Allen and Dynes indicates that the sample's T_c remains unchanged with respect to the observation angle, along with nearly constant electron-E_{2g} phonon coupling calculated from the Gaussian linewidth. Thus, despite the primary electron-phonon mechanism for the superconducting properties in MgB_2 arising from the E_{2g} phonon mode, T_c itself cannot be solely determined by electron-E_{2g} phonon coupling but also involves other yet-to-be-revealed phonon modes ω_1 and ω_3.

ACKNOWLEDGMENT

This work was supported by the Basic Science Research Program of the National Research Foundation of Korea (NRF) funded by the Ministry of Education (2021R1I1A3044518)

REFERENCES

[1] J. Nagamatsu, N. Nakagawa, T. Muranaka, Y. Zenitani and J. Akimitsu, Superconductivity at 39 K in Magnesium Diboride, *Nature* 410, 63-64, Mar. 2001.

[2] H. J. Choi, D. Roundy, H. Sun, M. L. Cohen, and S. G. Louie, The Origin of the Anomalous Superconducting Properties of MgB_2, *Nature* 418, 758, Aug. 2002.

[3] J. Kortus, I. I. Mazin, K. D. Belashchenko, V. P. Antropov, and L. L. Boyer, Superconductivity of Metallic Boron in MgB_2, *Phys. Rev. Lett.* 86, 4656, May 2001.

[4] J. M. An, and W. E. Pickett, Superconductivity of MgB_2: Covalent Bonds Driven Metallic, *Phys. Rev. Lett.*86, 4366, May 2001.

[5] K. P. Bohnen, R. Heid, and B. Renker, Phonon Dispersion and Electron-phonon Coupling in MgB_2 and A_1B_2, *Phys. Rev. Lett.* 86, 5771, June 2001.

[6] T. Yildirim, O. Gülseren, J. W. Lynn, C. M. Brown, T. J. Udovic, Q. Huang, N. Rogado, K. A. Regan, M. A. Hayward, J. S. Slusky, T. He, M. K. Haas, P. Khalifah, K. Inumaru, and R. J. Cava, Giant Anharmonicity and Nonlinear Electron-Phonon Coupling in MgB_2: A Combined First-Principles Calculation and Neutron Scattering Study, *Phys. Rev. Lett.* 87, 037001, June 2001.

[7] A. Y. Liu, I. I. Mazin, and J. Kortus, Beyond Eliashberg Superconductivity in MgB_2: Anharmonicity, Two-Phonon Scattering, and Multiple Gaps, *Phys. Rev. Lett.* 87, 087005, Aug. 2001.

[8] Y. Kong, O. V. Dolgov, O. Jepsen, and O. K. Andersen, Electron-phonon Interaction in The Normal and Superconducting States of MgB_2, *Phys. Rev. B* 64, 020501, May 2001.

[9] E. Nishibori, M. Takata, M. Sakata, H. Tanaka, T. Muranaka, and J. Akimitsu, Bonding Nature in MgB_2, *J. Phys. Soc. Jpn*. 70, pp. 2252-2254, May 2001.

[10] K. Kunc, I. Loa, K. Syassen, R. K. Kremer and K. Ahn, MgB_2 under Pressure: Phonon Calculations, Raman Spectroscopy, and Optical Reflectance, *J. Phys.: Condens. Matter* 13, pp 9945-9962, Oct. 2001.

[11] W. X. Li, Y. Li, H. R. Chen, R. Zeng, S. X. Dou, M. Y. Zhu, and H. M. Jin, Electron-phonon Interaction in the Normal and Superconducting States of MgB_2, *Phys. Rev. B* 77 094517, March 2008.

[12] W. X. Li, Y. Li, H. R. Chen, R. Zeng, M. Y. Zhu, H. M. Jin and S. X. Dou, Electron–phonon Coupling Properties in MgB_2 Observed by Raman Scattering, *J. Phys.: Condens. Matter* 20 255235, May 2008.

[13] R.P. Putra, Y.S. Lee, P. Duong, Y.J. Ko, W.N. Kang, K.-H. Kim, and B. Kang, Electron-phonon Coupling Behavior in MgB2 Films with Various Thicknesses of ZnO Buffer Layer on Metallic Substrates, *Solid State Commun*. vol. 323, 114117, Jan. 2021.

[14] X. Zheng, A. V. Progebnyakov. A. Kotcharov, J. E. Jones, X. X. Xi, E. M. Lysczek, J. M. Redwing, S. Xu, Q. Li, J. Lattieri, D. G. Schlom, W. Tian, X. Pan, and Z-K. Liu, In situ Epitaxial MgB_2 Thin Films for Superconducting Electronics, *Nature Materials*, 1, pp. 35-38, Sept. 2002.

[15] W. K Seong, S. Oh, and W. N. Kang, Perfect Domain-lattice Matching between MgB_2 and Al_2O_3 Single-crystal MgB_2 Thin Films Grown on Sapphire, *Jpn. J. Appl. Phys.* 51, 083101, July 2012.

[16] A. A. Baker, L. B. Bayu Aji, J. H. Bae, E. Stavrou, J. L. Beckham, S. K. McCall, and S. O. Kucheyev, Control of Superconductivity in MgB2 by Ion Bombardment, J. Phys. D: Appl. Phys. 52, 295302, May 2019.

[17] A. A. Baker, L. B. Bayu Aji, J. H. Bae, E. Stavrou, D. J. Steich, S. K. McCall and S. O. Kucheyev, Vapor Annealing Synthesis of non-Epitaxial MgB_2 Films on Glassy Carbon, *Supercond. Sci. Technol.* 31, 055006, March 2018

[18] P. M. Rafailov, S. Bahrs, and C. Thomsen, The Raman Spectra of MgB2 and Its Potential Impurity Phases, *Phys. Stat. Sol. (b)* 226, No. 2, R9-R11, June 2011

[19] B. Xu, N. Mao, Y. Zhao, L. Tong, and J. Zhang, Polarized Raman Spectroscopy for Determining Crystallographic Orientation of Low-Dimensional Materials, *J. Phys. Chem. Lett*. 12, pp. 7442-7452, Aug. 2021.

[20] Y. Zhao, S. S. Zhang, Y. P. Shi, Y. F. Zhang, R. Saito, J. Zhang, L. M. Tong, Characterization of Excitonic Nature in Raman Spectra Using Circularly Polarized Light, *ACS Nano* 14, 10527−10535, Aug. 2020.

[21] D. L. Rousseau, R. P. Bauman, and S. P. S. Porto, Normal Mode Determination in Crystals, *J. Raman Spectrosc*. vol 10, 1, pp. 253-290, Jan. 1981.

[22] L. Du, J. Tang, Y. Zhao, X. Li, R. Yang, X. Hu, X. Bai, X. Wang, K. Watanabe, T. Taniguchi, D. Shi, G. Yu, X. Bai, T. Hasan, G. Zhang and Z. Sun, Lattice Dynamics, Phonon Chirality and Spin-Phonon Coupling in 2D Itinerant Ferromagnet Fe_3GeTe_2, *Adv. Funct. Mater.* 29, 1904734, Sept. 2019.

[23] R. Loudon, The Raman effects in Crystals, *Adv. Phys*, vol.50, no. 7 pp. 813-864, Oct. 2001.

[24] V. Heine, Group Theory in Quantum Physics, 3rd ed, vol. 9. Pergamon Press, 1970, pp. 304-310

[25] W. L. McMillan, Transition Temperature of Strong-Coupled Superconductor, *Phys. Rev*. 167, 331, March 1968.

[26] P. B. Allen, and R.C. Dynes, Transition Temperature of Strong-Coupled Superconductor Reanalyzed, *Phys. Rev. B.* 12, 905, Aug. 1975.

[27] A. Brinkman, A. A. Golubov, H. Rogalla, O. V. Dolgov, J. Kortus, Y. Kong, O. Jepsen, and O. K. Andersen, Multiband model for Tunneling in MgB_2 Junction, *Phys. Rev. B*. 65, 180517(R), May 2002.

[28] G. Blumberg, A. Mialitsin, B. S. Dennis, N. D. Zhigadlo, and J. Karpinski, Multi-gap Superconductivity in MgB_2: Magneto-Raman Spectroscopy, *Physica C*, 456, pp. 75-82, Feb. 2007.

[29] G. Blumberg, A. Mialitsin, B. S. Dennis, M. V. Klein, N. D. Zhigadlo, and J. Karpinski, Observation of Legget's Collective Mode in a Multiband MgB_2 Superconductor, *Phys. Rev. Lett*. 99, 227002, Nov. 2007.

[30] A. Mialitsin, B. S. Dennis, N. D. Zhigadlo, J. Karpinski and G. Blumberg, Anharmonicity and Self-energy Effects of the E_{2g} Phonon in MgB_2, *Phys. Rev. B.* 75. 020509, Jan. 2007.

[31] P. B. Allen, Neutron Spectroscopy of Superconductors, *Phys. Rev. B*. 6, 2577, Oct. 1972